**NASA TECHNICAL NOTE**

NASA TN D-4959

C. 1

NASA TN D-4959

# HEAT-TRANSFER COEFFICIENTS FOR HYDROGEN FLOWING THROUGH PARALLEL HEXAGONAL PASSAGES AT SURFACE TEMPERATURES TO 2275 K

*by Jack G. Slaby and William F. Mattson*

*Lewis Research Center*

*Cleveland, Ohio*

NATIONAL AERONAUTICS AND SPACE ADMINISTRATION • WASHINGTON, D. C. • DECEMBER 1968

NASA TN D-4959

# HEAT-TRANSFER COEFFICIENTS FOR HYDROGEN FLOWING

# THROUGH PARALLEL HEXAGONAL PASSAGES

# AT SURFACE TEMPERATURES TO 2275 K

By Jack G. Slaby and William F. Mattson

Lewis Research Center
Cleveland, Ohio

NATIONAL AERONAUTICS AND SPACE ADMINISTRATION

## ABSTRACT

Local forced-convection heat-transfer data are presented for hydrogen flowing through an electrically heated test section composed of 19 hexagonal parallel passages with a length- to equivalent-diameter ratio of 63.5. The data cover ranges of surface- to hydrogen-temperature ratios from 1.43 to 3.38, bulk Reynolds numbers from 12 950 to 21 960, surface temperatures to 2275 K, and outlet hydrogen temperatures to 747 K. The results are correlated in terms of Nusselt, Prandtl, and modified Reynolds numbers. The data fell within about ±20 percent of the correlating equations. The heat-transfer results agreed with those obtained from a parallel flat-plate test section with similar dimensions.

# HEAT-TRANSFER COEFFICIENTS FOR HYDROGEN FLOWING THROUGH PARALLEL HEXAGONAL PASSAGES AT SURFACE TEMPERATURES TO 2275 K

by Jack G. Slaby and William F. Mattson

Lewis Research Center

## SUMMARY

Local forced-convection heat-transfer data are presented for hydrogen flowing through a direct-current resistance-heated test section that is composed of 19 hexagonal parallel passages and has a length- to equivalent-diameter ratio of 63.5. The experimental data cover ranges of surface- to hydrogen-temperature ratios from 1.43 to 3.38, bulk Reynolds numbers from 12 950 to 21 960, surface temperatures to 2275 K, and outlet hydrogen temperatures to 747 K corresponding to an exit Mach number of 0.9 at pressures slightly above 1 atmosphere. The inlet hydrogen temperature was constant at 294 K. The heat-transfer results are presented and correlated by modified Dittus-Boelter equations with hydrogen gas properties evaluated at the bulk, film, and surface temperatures. The data fell within about ±20 percent of the correlating equations.

The heat-transfer results agreed with those obtained from a parallel-flat-plate test section with a similar equivalent diameter and the identical length and flow rate. This comparison was made for various power inputs.

## INTRODUCTION

Flowing hot gas has been used to evaluate fuel-element designs out-of-pile. The design and operation of gas heaters capable of heating hydrogen, helium, and nitrogen to temperatures above 2500 K are reported in references 1 to 3. Gas was heated by flowing over or through electric, resistance-heated, tungsten heating elements in the form of either parallel flat plates or interwoven mesh. A tungsten honeycomb structure, consisting of parallel hexagonal passages, was also considered for use as a heater element and as a fuel element for a gas-cooled nuclear reactor. Evaluating the honeycomb required special fabrication so that it could be subjected to direct-current resistance heating. One honeycomb was fabricated so that the flow area, equivalent diameter, length, and electri-

cal resistance were about the same as one stage of the parallel flat-plate test section described in reference 2. The two types of test sections, hexagonal-passage and flat-plate, are shown in figures 1 and 2, respectively. Heat-transfer tests with axial temperature gradients were conducted on the hexagonal-passage honeycomb test section at conditions similar to those used for the parallel flat-plate test section reported in reference 1.

This report correlates the local hydrogen heat-transfer coefficients, obtained from the honeycomb test section, in terms of Nusselt number, Prandtl number, and modified Reynolds number. Hydrogen gas properties are evaluated at bulk, film, and surface temperatures for the different correlations.

The same local hydrogen heat-transfer coefficients are also compared with the heat-transfer coefficients obtained from the parallel flat-plate test section described in reference 1. The heat-transfer coefficients are expressed in terms of Nusselt numbers.
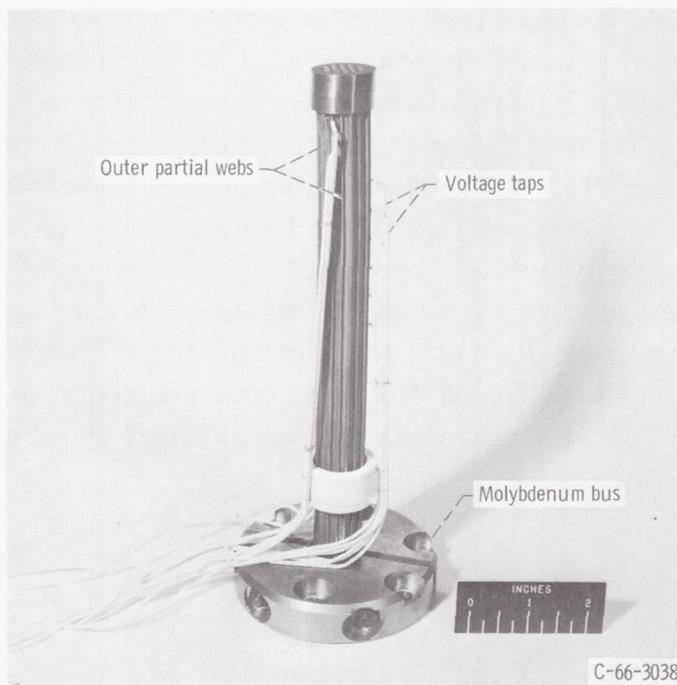


Figure 1. - Hexagonal-passage tungsten test section instrumented with voltage taps.

Spacer-supported tungsten flat-plate test section of reference 2.

Tungsten plate test section

Boron nitride housing

Voltage tap leads

C-67-1861
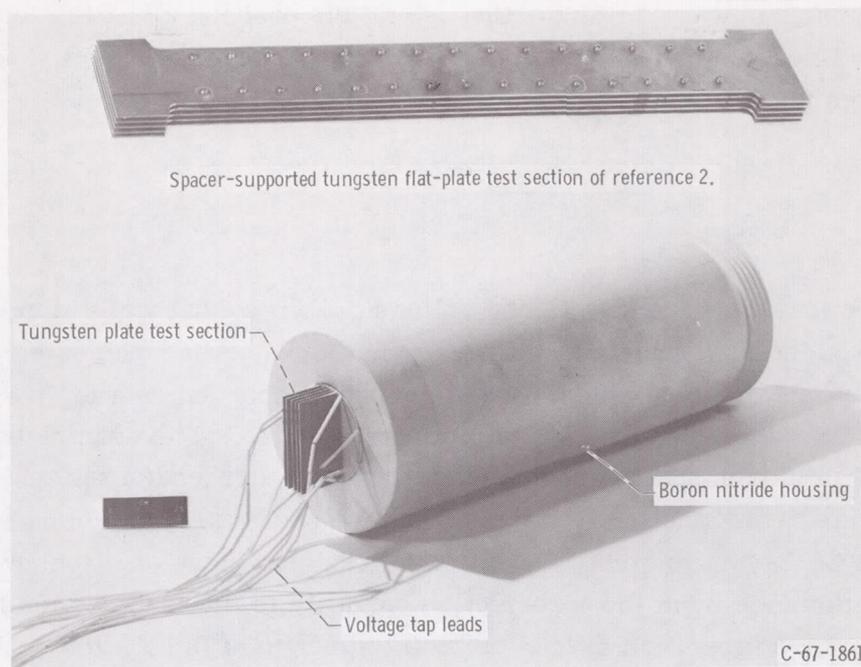
Figure 2. - Assembled flat-plate test section.

# TEST SECTION

## Description

Heat-transfer experiments were performed on the tungsten honeycomb test section shown in figure 1. The honeycomb, fabricated by a powder-metallurgy sintering process, has a density of about 98 percent of theoretical, as measured by a mercury porosimeter. The overall honeycomb length is 23.5 centimeters, and a 1.905-centimeter-diameter circle would encompass the test-section periphery. The circular ends serve as electrical bus connections and are an integral part of the honeycomb. The test-section length between buses, the power generation length, was 20.3 centimeters. The honeycomb test section consisted of 72 inner webs forming 19 hexagonal passages and 14 outer partial webs attached to the periphery. These outer webs (the result of the manufacturing process) are incomplete hexagonal passages and provided a means for attaching the voltage taps. The maximum variation between any of the three across-the-flat measurements for a given passage was not more than 0.254 millimeter. The average flat-to-flat distance for the 19 passages of the honeycomb heater was 3.20 millimeters. The variation in passage equivalent diameter was ±0.051 millimeter from the average equivalent diameter of 3.20 millimeters. The average web thickness was 0.548 millimeter.

These dimensional variations occurred only in the radial direction. In the axial di-

3

rection, the dimensions were uniform, that is, at any position along the test-section length, a given dimension was constant. The total tungsten cross section was therefore constant along the test-section length.

## Instrumentation

The test section was instrumented by voltage tap wires that were attached to the honeycomb through holes disintegrated by electric discharge into the outer partial webs, as shown in figure 1. Readings from these taps were recorded on a digital voltmeter and were later used to determine surface temperature profiles. The spacing of the voltage taps was varied; a closer spacing was used near the hot exit end of the test section to allow more accurate determination of the temperature profiles. The voltage taps were placed along the 20.3-centimeter test-section length, and these positions were designated as ratios of the distance from the test-section entrance to the test-section length $x/L$. The first four voltage taps were spaced at $x/L$ intervals of 0.125, the next six at 0.0625, and the last four at 0.03125. The voltage profiles are shown in figure 3. The current flowing through the test section was measured by a calibrated shunt.

The test section was mounted in the test facility described in reference 2. The heater inlet gas temperature $T_i$ was measured by a Chromel-Alumel thermocouple and was 294 K for each of the four runs. A choked-flow nozzle was used to measure the gas flow rate, which was set by adjusting the nozzle inlet pressure at room temperature.
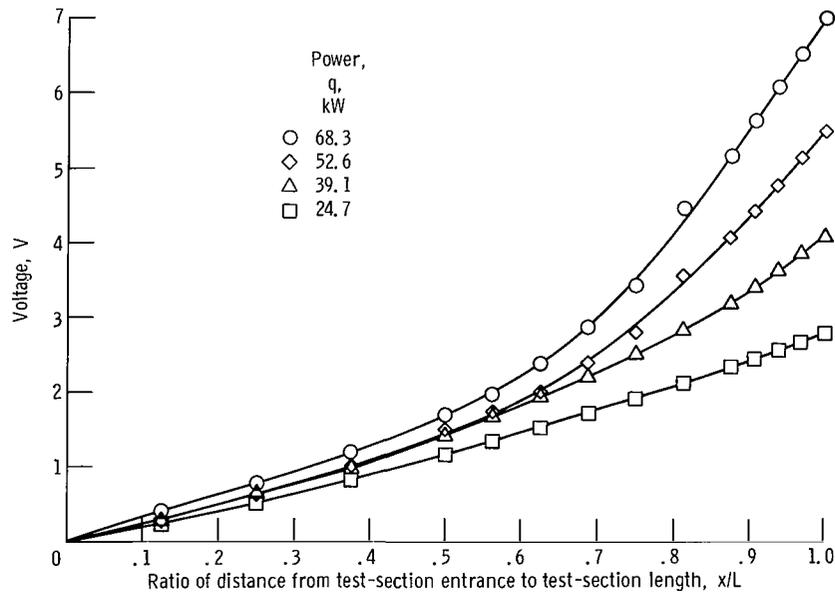


Figure 3. - Comparison of voltage profiles from hexagonal-passage test section for various amounts of power input. Hydrogen mass flow rate, 10.44 grams per second.

4

Constant gas flow could be maintained provided that the exit pressure was not raised sufficiently to unchoke the nozzle. The exit pressure was maintained slightly above 1 atmosphere. A heat balance on a hydrogen-to-water heat exchanger, located at the test-section exit, was used as a means of obtaining the outlet gas temperature. The heat-exchanger water flow rate $W_{H_2O}$ was measured with an orifice and the water temperature rise $\Delta T_{H_2O}$ with a differential iron-constantan thermocouple. A detailed description of the flowing gas facility used, including the instrumentation, is given in reference 2.

## METHOD OF CALCULATION

Forced-convection heat-transfer coefficients were calculated from the data for hydrogen flowing through an electrically heated test section, which was composed of 19 hexagonal passages and had a length- to equivalent-diameter ratio of 63.5, based on the test-section length of 20.3 centimeters and the average equivalent diameter of 3.20 millimeters. Local coefficients were calculated because the surface temperature, heat flux, and gas temperature varied significantly along the axial length of the test section. One hydrogen mass flow rate was used, and the electrical power to the test section was varied to change the heat-transfer coefficient.

### Wall Temperature Profiles

The wall temperature profiles were obtained in the following manner: Readings from voltage taps, attached along the honeycomb length, were used to plot the voltage profiles shown in figure 3. From the profiles, incremental voltages $\Delta V$ corresponding to incremental test-section lengths $\Delta L$ were taken. The $\Delta L$ chosen for these calculations was 2.03 centimeters, which divided the honeycomb test section into 10 equal parts. The current $I$ through the honeycomb cross-sectional area $A_c$ was measured. The local resistivity $\zeta$ of the tungsten test section can then be calculated by

$$\zeta = \frac{\Delta V}{I} \frac{A_c}{\Delta L}$$

(All symbols are defined in appendix A.) The average incremental test-section surface temperature was determined from a plot of tungsten resistivity as a function of temperature, as given in reference 4.

The calculated incremental surface temperature $T_s$ is plotted in figure 4 as a function of test-section length
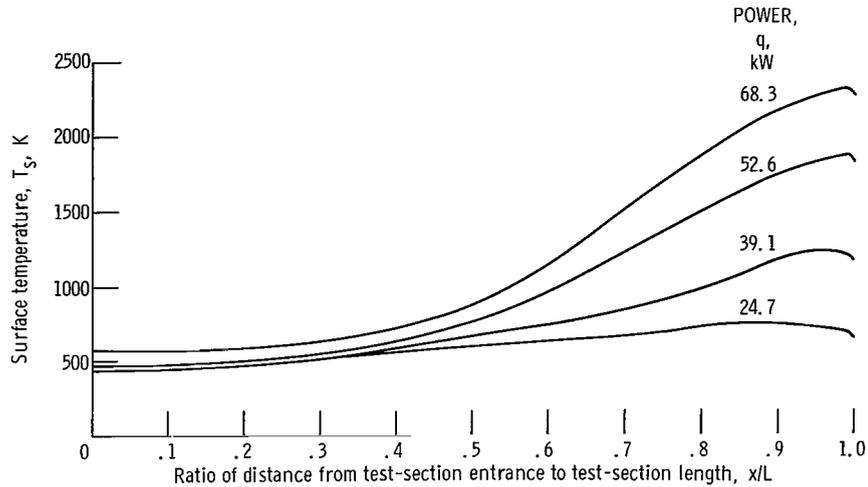
Figure 4. - Comparison of calculated surface temperature profiles from hexagonal-passage test section for various amounts of power input. Hydrogen mass flow rate, 10.44 grams per second.

## Test-Section Heat Balance

The internal heat generated in a test-section increment $\Delta L$ equals the amount of heat added to the flowing hydrogen (see assumptions in RESULTS AND DISCUSSION section). Thus, for each of the 10 increments from $x/L = 0$ to $x/L = 1.0$, the following equation can be written:

$$\Delta q = \Delta VI = W(H_o - H_i)$$

where $\Delta V$ can be read directly from the voltage profiles in figure 3 and the current obtained from the tabulation in table I. With the gas flow rate $W$ known, the change in enthalpy $\Delta H$ of the gas flowing along an increment can be calculated. After $\Delta H$ is calculated for the first increment and the heater inlet gas temperature $T_i$ is measured, the outlet gas temperature from the first increment can be determined from the hydrogen enthalpy-temperature tables of reference 5. The outlet gas temperature from this first increment becomes the inlet gas temperature for the second or adjacent downstream increment. After the 10 increments are treated in this manner, the test-section outlet gas temperature $T_o$ is finally determined. The bulk temperature per increment was calculated as the arithmetic average of the inlet and exit gas temperatures for each increment. A plot of the gas temperature as a function of test-section length for various power inputs is presented in figure 5. The outlet gas temperature for each run is tabulated in table I. These temperatures were determined by assuming that all the heat generated in the test section was added to the hydrogen. The validity of this assumption was tested by com-

6

## TABLE I. - TEST-SECTION PARAMETERS AND DATA

(a) Hexagonal-passage test section. Cross-sectional area of current flow, $A_c$, 0.927 square centimeter; free-flow area, $A_f$, 1.66 square centimeters; surface area, $A_s$, 426 square centimeters; equivalent diameter, $D_e$, 3.2 millimeters; test-section length, L, 20.3 centimeters; hydrogen inlet temperature, $T_i$, 294 K; gas flow rate, W, 10.44 grams per second

| Run | Voltage across test section, V | Current through test section, I, A | Outlet gas temperature, $T_o$, K | Power generated in test section, q, kW |
|---|---|---|---|---|
| 1 | 2.79 | 8850 | 454 | 24.7 |
| 2 | 4.07 | 9600 | 551 | 39.1 |
| 3 | 5.49 | 9600 | 644 | 52.6 |
| 4 | 6.97 | 9800 | 747 | 68.3 |

(b) Parallel flat-plate test section. Equivalent diameter, $D_e$, 0.285 centimeter; test-section length, L, 20.3 centimeters

| Run | Voltage across test section, V | Current through test section, I, A | Outlet gas temperature, $T_o$, K | Power generated in test section, q, kW |
|---|---|---|---|---|
| 900 | 3.38 | 10 800 | 530 | 36.5 |
| 901 | 6.20 | 11 800 | 742 | 73.1 |
| 902 | 8.60 | 12 000 | 903 | 103.1 |
| 905 | 11.70 | 12 400 | 1136 | 145.0 |
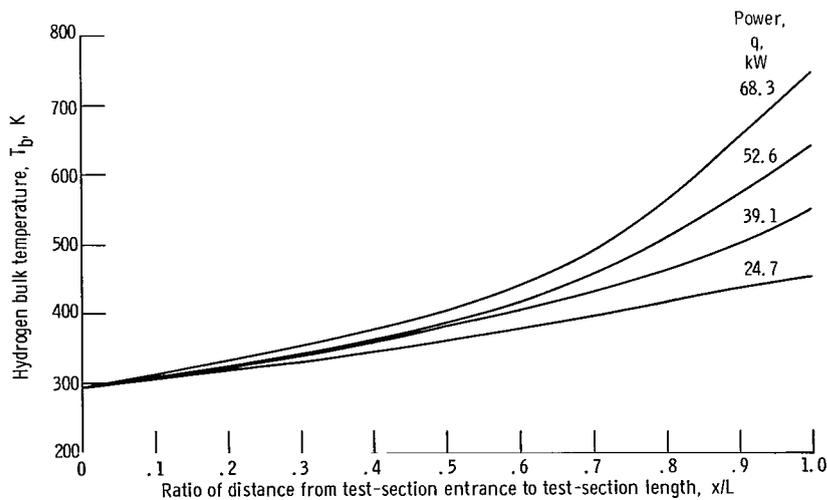


Figure 5. - Calculated hydrogen bulk temperature profiles from hexagonal-passage test section as function of passage length for various amounts of power input. Hydrogen mass flow rate, 10.44 grams per second.

paring the calculated test-section outlet gas temperature with the gas temperature determined by a heat balance on the hydrogen-to-water heat exchanger located at the test-section exit. This calculation was possible because the temperature of the gas leaving the test section did not drop a significant amount before the gas entered the heat exchanger. Thus, the heat balance on the hydrogen-to-water heat exchanger could be expressed

$$W_{H_2}(C_p)_{H_2}(T_o - T_g) = W_{H_2O}(C_p)_{H_2O}\Delta T_{H_2O}$$

$$T_o = \frac{W_{H_2O}(C_p)_{H_2O}\Delta T_{H_2O}}{W_{H_2}(C_p)_{H_2}} + T_g$$

Specific heat values for hydrogen were taken from reference 6. The balance between the heat picked up by the heat exchanger and the heat generated in the test section did not differ by more than ±10 percent. Thermocouples were not used to measure the exit gas temperature because prior tests conducted with thermocouples and melting plugs showed that the heat-balance method of calculating an exit gas temperature was satisfactory.

## Heat-Transfer Geometry Factors

The values of the honeycomb test-section parameters, such as the equivalent diameter $D_e$, the free-flow area $A_f$, the surface area $A_s$, and the tungsten cross-sectional area $A_c$, were based on average values because the honeycomb transverse dimensions were not uniform. A shadowgraph of the honeycomb cross section (×10) was used to measure the individual dimensions of the passages and webs. These measurements were used to calculate the geometric parameters.

For each hexagonal passage, the equivalent diameter $D_e$, which is equal to the distance across flats for a symmetrical hexagon, was obtained by averaging the three flat-to-flat dimensions. The maximum flat-to-flat variation for a given passage was not more than 0.254 millimeter, and the average equivalent diameter for the 19 passages was 3.200±0.051 millimeters.

The free-flow area $A_f$ on the shadowgraph was measured with a planimeter. As a check, the free-flow area was calculated on the basis of the average equivalent diameter of 3.20 millimeters. Hence,

$$A_f = 19N\left(\frac{D_e}{2}\right)^2 \tan 30^{\circ}$$

where the number of sides per passage N is 6. The planimeter measurement and the calculated value checked within 2 percent of each other.

The surface area $A_s$ of a regular hexagonal passage was calculated by

$$A_s = NLD_e \tan 30^{\circ}$$

In addition, the calculated value of the surface area was checked by using the measured wetted perimeter of the passages from the shadowgraph in the following expression:

$$A_s = (\text{Wetted perimeter}) \times (L)$$

The two values checked within 1/2 of 1 percent.

## Heat-Transfer Coefficient

The local heat-transfer coefficient per increment of length is then calculated by

$$h = \frac{\Delta q}{\Delta A_s (T_s - T_b)}$$

The physical properties of the Nusselt and Prandtl numbers, defined as $Nu = hD_e/k$ and $Pr = \mu C_p/k$, respectively, were evaluated at the bulk, the film, or the surface temperature. Values for viscosity $\mu$ and thermal conductivity $k$ were obtained from reference 7.

The modified Reynolds number (as discussed in ref. 8) was defined as

$$Re_y = \frac{GD_e}{\mu_y} \frac{T_b}{T_y}$$

where y was either the surface or the film temperature. The correlating equation used was of the form

$$(Nu)_y = 0.023(Re)_y^{0.8}(Pr)_y^{0.4}$$

Taylor (ref. 9) recommends using a heat-transfer correlation based on bulk proper-ties and including a surface- to bulk-temperature ratio $T_s/T_b$ raised to a power that is a function of the length- to equivalent-diameter ratio $L/D_e$. This correlation, based on tubes, covers a wide range of conditions, including surface- to fluid-bulk-temperature ratios to 23. This correlation is represented by

$$Nu_b = 0.023\ Re_b^{0.8}Pr_b^{0.4}\left[\left(\frac{T_s}{T_b}\right)\exp-\left(\frac{0.57-1.59}{\dfrac{x}{D_e}}\right)\right]$$

## RESULTS AND DISCUSSION

The basic heat-transfer results of this investigation were obtained from a 19-parallel-hexagonal-passage tungsten test section with power generation resulting from direct-current resistance heating. Although this honeycomb was used as a heat-transfer test section, several features (discussed in appendix B) indicate its potential as a heater to supply hot gases.

### Restrictions and Assumptions

One hydrogen mass flow rate was used, and the electrical power to the test section was varied to change the heat-transfer coefficient. The correlating parameters were cal-culated from the experimental data. As is true with most correlations, there were cer-tain restrictions and assumptions under which the experimental data were used to calcu-late the heat-transfer parameters. These restrictions and assumptions are

(1) Steady-state conditions are assumed.

(2) The static pressure drop across each of the 19 passages is the same. Because all the passages are not uniform in flow area, the hydrogen flow will readjust so that the sum of friction and momentum pressure drop in each passage remains constant for a given power setting.

(3) Axial conduction is negligible. For the most extreme temperature profile, the difference between the heat conducted into an increment and the heat conducted out of an increment is less than 1 percent of the total internal heat generated per increment.

(4) Radiation loss is negligible. The outer surface of the honeycomb radiated to the containment vessel walls. This radiation loss is approximately 1 percent of the total heat generated. Even for the high-power run (run 4, see table I), a calculated radiation loss from the highest temperature increment was less than 5 percent of the heat generated in that increment.

(5) All the heat generated in the 20.3-centimeter test-section length is transferred to the gas flowing through the hexagonal passages.

(6) At any particular axial position along the hexagonal passage, the transverse surface temperature remains constant. Or stated differently, the wall temperature for a given power level varies only in the axial direction. The validity of this statement is based on several self-correcting effects. Radiation heat transfer between hexagonal faces as well as transverse conduction between webs tends to keep the webs at a uniform temperature. In addition, webs that tend to run cooler have lower electrical resistivity, and, consequently, more current can flow in these webs. As a result, the additional current tends to raise the surface temperature.

(7) The individual passages did not vary along the length of the test section. Post-test inspection of sectioned portions of the heater showed that variations in equivalent diameter from passage to passage at any given axial position remained constant along the passage length.

(8) No attempt was made to modify the heat-transfer coefficients for sharp-corner effects. Reference 10 shows these effects to be secondary in a honeycomb.

(9) The density of the tungsten honeycomb heater was about 98 percent of theoretical. No correction was applied to the resistivity-temperature relation of tungsten in the calculation of the wall temperature profiles.

## Nonuniform Passage Effect

The significant test-section dimensions are given in table I along with appropriate test data for both hexagonal-passage and parallel flat-plate test sections. The information from table I, when used in conjunction with the voltage profiles of figure 3 and the tungsten temperature-resistivity relation presented in reference 4, is sufficient to make the heat-transfer calculations of this investigation.

However, before the heat-transfer data are discussed, it is important to determine whether or not the variation in equivalent diameter between individual passages ($D_e$ = 3.200±0.051 mm) has a significant effect on the heat-transfer results. Consequently, a calculation was made, based on inlet and exit conditions. A severe, but highly unlikely, condition was considered in which one small passage ($D_e$ = 3.15 mm) was surrounded by six passages with an equivalent diameter equal to the average, $D_e$ = 3.20 mil-

limeters. The calculation was subject to the same assumptions discussed earlier in this section; that is, constant static pressure drop across all the passages and constant wall surface temperature at a particular axial position. The heat-transfer surface area per passage is proportional to the passage equivalent diameter, and the passage free-flow area is proportional to the square of the equivalent diameter.

Under these conditions, the calculated difference in the average heat flux (heat transferred per unit surface area) between the small and average size passages for run 4 (the high-power run) is less than 1 percent. The heat transferred between passages is not the same: the variation is about 2 percent. Under the conditions of this investigation, the heat-transfer coefficient is approximately proportional to the heat flux. Therefore, the conclusion was that the variation in equivalent diameter was not a significant factor in the heat-transfer results of this investigation. However, as described in reference 11, cases exist where the heat generated per passage remains constant (nuclear rocket application) and variations in equivalent diameter can cause significant surface temperature variations.

## Heat-Transfer Correlations

The local heat-transfer coefficients of the honeycomb were calculated from the wall surface temperature profiles shown in figure 4. For the hexagonal-passage test section, the value of $L/D_e$ was 63.5. Ten equally spaced increments were chosen along the length of the test section to calculate the local heat-transfer coefficients. The values of the ratio $x/D_e$ ranged from 3.17 (at the center of the first increment) to 60.3 (at the center of the last increment). Ten local heat-transfer coefficients were calculated for each of the four different power inputs to the test section. The test runs are characterized by the power input to the heater. The maximum exit Mach number was 0.9.

Hexagonal and flat-plate test data. - The first heat-transfer equation correlating the data consists of a modified Dittus-Boelter equation of the form

$$Nu_f = 0.023(Re_f)^{0.8}(Pr_f)^{0.4}$$

where the hydrogen physical properties are evaluated at the film temperature. This method of correlation was used to compare the heat-transfer results of the hexagonal-passage data with those obtained from the parallel flat-plate data of reference 1. The parallel flat-plate data correlated best with the Dittus-Boelter equation when the mass velocity was based on the minimum cross-sectional flow area (at a position where the plate supporting spacers were located). In addition, the surface area of the 10 sets of spacers exposed to the hydrogen was used as part of the heat-transfer surface area.

Thus, the modified film Reynolds number (given in ref. 8) was calculated as

$$\frac{G_{max}D_e}{\mu_f}\frac{T_b}{T_f}$$

and the correlating equation was

$$Nu_f = 0.023(Re_f)^{0.8}(Pr_f)^{0.4}$$

All the honeycomb data fell within a band of +17 and -22 percent of this film correlation.

The hydrogen mass flow rate through both test sections was identical, and the $L/D_e$ and equivalent diameter of both test sections were similar (see table I). However, a comparison of the local turbulent heat-transfer coefficients in figures 6(a) and (b) shows that the honeycomb data fell below the flat-plate spacer-supported data. Possibly the hydrogen flow around the 10 sets of spacers increased the turbulence sufficiently to cause the flat-plate data to fall higher than that of the honeycomb. In figure 7, the honeycomb data were plotted by using a modified Reynolds number based on the honeycomb surface temperature; and the hydrogen physical properties were evaluated at the surface temperature. The data fall in a more orderly trend around the correlating line, which is represented by



(a) Test section consisting of 19 parallel hexagonal passages. Correlating line, $Nu_f = 0.023\ Re_f^{0.8}Pr_f^{0.4}$.

(b) Test section consisting of five flat plates separated by spacers (ref. 1). Correlating line, $Nu_f = 0.023[(G_{max}D_e/\mu_f)(T_b/T_f)]^{0.8}Pr_f^{0.4}$.
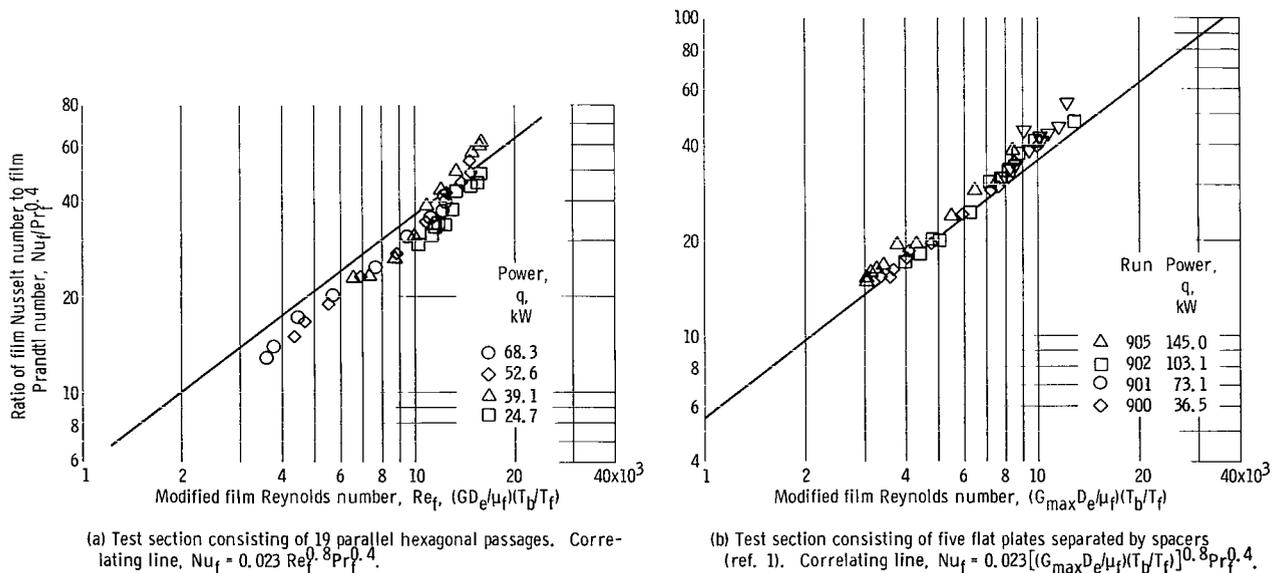
Figure 6. - Correlation of local turbulent heat-transfer coefficients. Hydrogen mass flow rate, 10.44 grams per second.
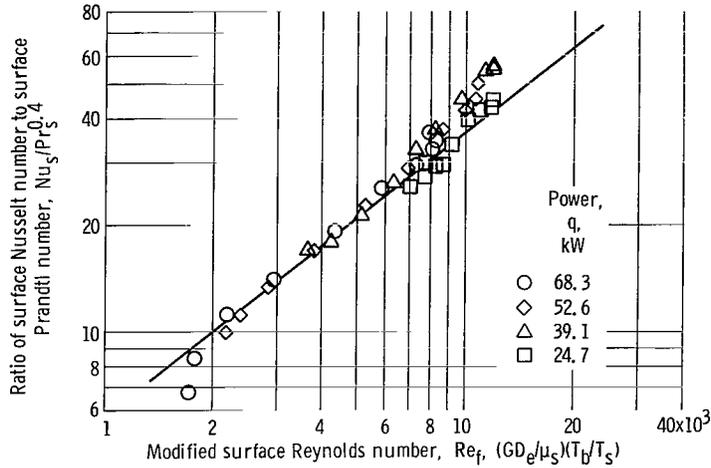
Figure 7. - Correlation of local turbulent heat-transfer coefficients. Hydrogen mass flow rate, 10.44 grams per second; test section consisted of 19 parallel hexagonal passages. Correlating line, $Nu_s = 0.023 Re_s^{0.8} Pr_s^{0.4}$.

the following equation given in reference 8:

$$Nu_s = 0.023 \left(\frac{GD_e}{\mu_s}\right)^{0.8} \left(\frac{T_b}{T_s}\right)^{0.8} (Pr_s)^{0.4}$$

Eighty-five percent of the data fall within a band of +20 and -10 percent of this correlating line. Of even more significance is the fact that the points which deviate the most from the correlating line are either test-section entrance points, where the amount of heat transferred is low, or test-section exit points, where the surface temperature is high. Points away from both the entrance and exit regions correlate well with the modified surface Reynolds number equation. Apparently, the heat-transfer results from parallel flow in 19 hexagonal passages, as well as results from flow between five parallel flat plates supported by spacers, correlate well when the smooth-tube correlations of reference 8 are used.

Figures 8 and 9 are based on the data of run 4, the high-power run, and illustrate the typical axial variation of the significant heat-transfer parameters for a given gas flow rate. The similarity between the shapes of the incremental heat-transfer rate (incremental heat generation rate) and the curves of the honeycomb surface temperature occurs because the electrical resistivity of tungsten varies almost linearly with temperature. For a given run, the current is constant, and the incremental heat generation varies as the tungsten resistivity.

The decrease in the modified surface Reynolds number from inlet to exit is a

14
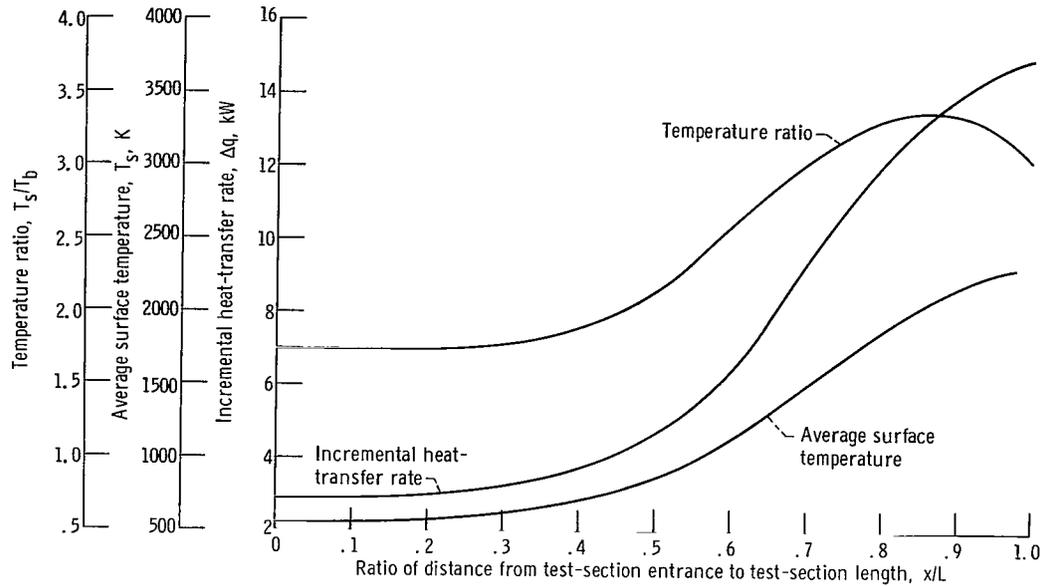
Figure 8. - Typical variation of temperatures and heat-transfer rate with test-section length. Hydrogen mass flow rate, 10.44 grams per second, power input, 68.3 kilowatts; test section consisted of 19 parallel hexagonal passages.
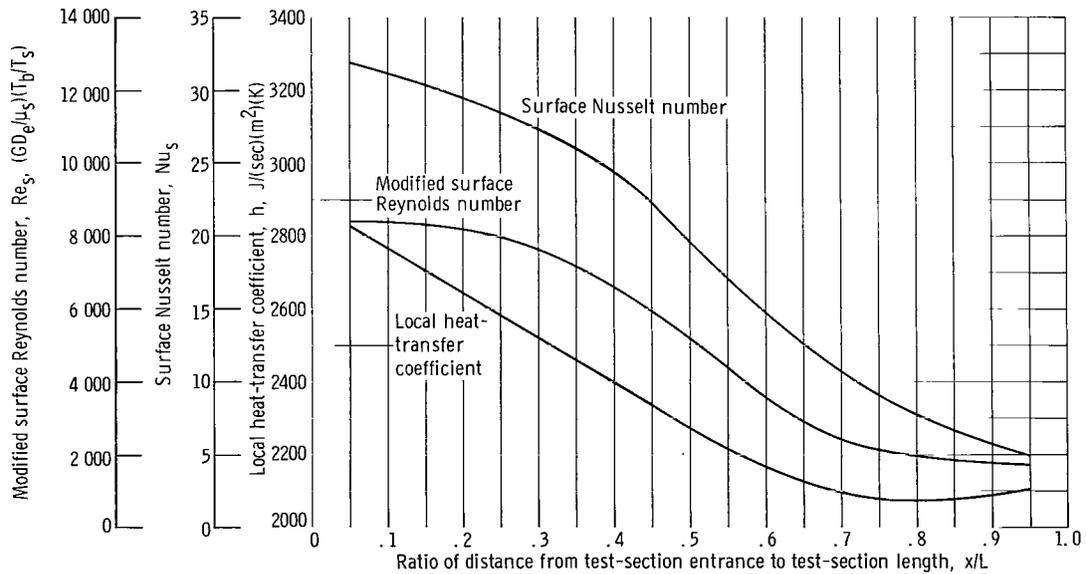


Figure 9. - Typical variation of Reynolds number, Nusselt number, and heat-transfer coefficient with test-section length. Hydrogen mass flow rate, 10.44 grams per second; power input, 68.3 kilowatts; test section consisted of 19 parallel hexagonal passages.

hydrogen-property effect influenced by the increase in hydrogen viscosity with temperature. Concurrent with this behavior is the inverse effect of the ratio $T_s/T_b$. This ratio begins to increase rapidly at an $x/D_e$ of about 0.45 and then levels off before decreasing near the test-section exit. The Nusselt number curve, with a slight variation due to a Prandtl number effect, varies in a manner similar to the shape of the modified surface Reynolds number curve.

Consider the heat-transfer coefficient along the test section. For a given equivalent diameter and constant hydrogen thermal conductivity, the heat-transfer coefficient would vary directly with the Nusselt number curve. This variation is shown over about half the test-section length. However, as the hydrogen thermal conductivity increases with temperature along the length of the test section (particularly along the latter half), the heat-transfer coefficient then varies directly with both the Nusselt number and the hydrogen thermal conductivity. The thermal conductivity of hydrogen, at about atmospheric pressure, increases rapidly with temperature, particularly at high temperatures. As a consequence, the heat-transfer coefficient levels off at $x/L$ of about 0.8 and begins to increase in the region near the test-section exit.

<u>Heat-transfer coefficient modified for effect of length- to equivalent-diameter ratio.</u> - For symmetrically heated straight tubes, Taylor (ref. 9) recommends a correlation line that will predict local single-phase forced-convection heat-transfer coefficients for turbulent flow over a much greater range of conditions than was previously possible. The correlation line that Taylor used for surface- to fluid-bulk-temperature ratios up to 23 is represented by

$$Nu_b = 0.023\ Re_b^{0.8} Pr_b^{0.4} \left[ \left( \frac{T_s}{T_b} \right) \exp - \left( 0.57 - \frac{1.59}{\dfrac{x}{D_e}} \right) \right]$$

where the Nusselt, Reynolds, and Prandtl numbers are all evaluated at the fluid bulk temperature but are modified by a ratio of surface to bulk temperature raised to a power that is a function of $x/D_e$, the distance along the test section.

The data of the present investigation, correlated with this equation, are shown in figure 10. Eighty-five percent of the data fall within ±15 percent of the correlating line. The points that deviate the most from the correlating line are the entrance points from the three higher power runs and some of the intermediate points from the low-power run. Nevertheless, all the data points fall within ±20 percent of the correlating line used by Taylor.
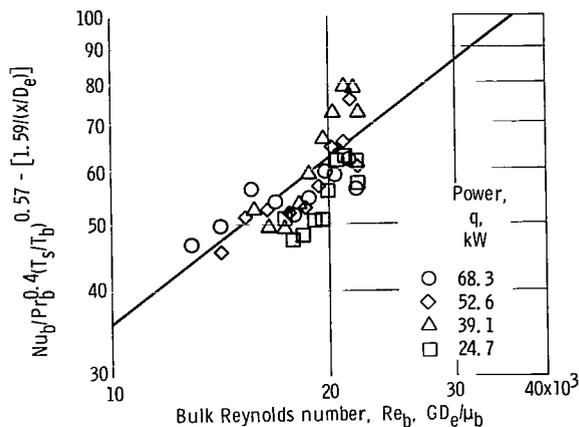
Figure 10. - Correlation of local heat-transfer coefficients by method of reference 9. Hydrogen mass flow rate, 10.44 grams per second. Test section consisted of 19 parallel hexagonal passages. Correlating line, $Nu_b = 0.023 Re_b^{0.8} Pr_b^{0.4} (T_s/T_b)^{-[0.57-1.59/(x/D_e)]}$.

# SUMMARY OF RESULTS

An investigation of heat transfer from parallel hexagonal passages to flowing hydrogen was conducted on a test section with a length- to equivalent-diameter ratio of 63.5. The data cover ranges of surface- to hydrogen-temperature ratios from 1.43 to 3.38, bulk Reynolds numbers from 12 950 to 21 960, surface temperatures to 2275 K, and outlet hydrogen temperatures to 747 K. The inlet hydrogen temperature was constant at 294 K, and the maximum exit Mach number was 0.9.

Local turbulent heat-transfer coefficients obtained experimentally from a 19-parallel-hexagonal-passage test section correlated when a modified Dittus-Boelter equation was used with hydrogen properties evaluated at the film, surface, and bulk temperatures.

The film and surface correlating equations were of the form

$$(Nu)_y = 0.023(Re)_y^{0.8}(Pr)_y^{0.4}$$

where y was either the film or surface temperature. All the data based on the film equation fell within +17 and -22 percent of the film correlating equation. Eighty-five percent of the data based on the surface equation fell within a band of +20 and -10 percent of the surface correlating equation.

The correlating equation based on bulk properties is represented by

$$Nu_b = 0.023 \, Re_b^{0.8} \, Pr_b^{0.4} \left[ \left( \frac{T_s}{T_b} \right) \exp - \left( 0.57 - \frac{1.59}{\dfrac{x}{D_e}} \right) \right]$$

This correlation is based on bulk properties and includes a surface- to fluid-bulk-temperature ratio $T_s/T_b$ raised to a power that is a function of the length- to equivalent-diameter ratio $x/D_e$. Eighty-five percent of the data fell within ±15 percent of this correlating line, and all the data fell within ±20 percent of it.

In this investigation, local heat-transfer coefficients, expressed in terms of the dimensionless parameters - Nusselt number, Prandtl number, and Reynolds number - showed good agreement when they were compared with the results obtained from a test section consisting of five parallel spacer-supported flat plates. The comparison was made for various power inputs. The hydrogen flow rate was identical in both tests, and the lengths of the test sections as well as the equivalent diameters were also approximately equal.

Lewis Research Center,
    National Aeronautics and Space Administration,
        Cleveland, Ohio, October 7, 1968,
            120-27-04-54-22.

# APPENDIX A

## SYMBOLS

$A_c$    cross-sectional area of current flow, $cm^2$

$A_f$    free-flow area, $cm^2$

$A_s$    surface area, $cm^2$

$\Delta A_s$    incremental surface area, $cm^2$

$C_p$    specific heat of hydrogen at constant pressure, $J/(g)(K)$

$D_e$    equivalent diameter, cm

$G$    mass velocity, $g/(sec)(cm^2)$

$G_{max}$    mass velocity at spacer cross section, $g/(sec)(cm^2)$

$H$    enthalpy, $(kW)(sec)/g$

$\Delta H$    change in enthalpy, $(kW)(sec)/g$

$h$    local heat-transfer coefficient, $J/(sec)(cm^2)(K)$

$I$    current, A

$k$    thermal conductivity of hydrogen, $J/(cm)(sec)(K)$

$L$    test-section length, cm

$\Delta L$    incremental test-section length, cm

$N$    number of sides per passage

$Nu$    Nusselt number, $hD_e/k$

$Pr$    Prandtl number, $C_p\mu/k$

$q$    rate of heat transfer to gas, kW

$\Delta q$    incremental rate of heat transfer to gas, kW

$Re_b$    Reynolds number, $GD_e/\mu_b$

$Re_f$    modified film Reynolds number, $(GD_e/\mu_f)(T_b/T_f)$

$Re_s$    modified surface Reynolds number, $(GD_e/\mu_s)(T_b/T_s)$

$T$    temperature, K

$\Delta T$    change in temperature, K

$\Delta V$    incremental voltage drop, V

$W$    gas flow rate, g/sec

$x$    distance from entrance of test section, cm

$\mu$    absolute viscosity of hydrogen, $g/(sec)(cm)$

$\zeta$    resistivity of tungsten, ohm-cm

Subscripts:

$b$    bulk (when applied to properties, indicates evaluation at average bulk temperature $T_b$)

$f$    film (when applied to properties, indicates evaluation at average film temperature $T_f$)

$g$    heat-exchanger exit gas

$H_2$    hydrogen

Subscripts:

$H_2O$    water

i      hydrogen inlet to test section

o      hydrogen outlet from test section

s      surface (when applied to properties, indicates evaluation at average surface temperature $T_s$)

y      indicates either film or surface temperature evaluation of properties

# APPENDIX B

## ADVANTAGES OF HONEYCOMB AS HOT-GAS HEATER OVER PARALLEL

## FLAT-PLATE AND MESH-TYPE HEATERS

The honeycomb test section was far easier to instrument with voltage taps along its length than were the parallel flat-plate heater (ref. 1) and the mesh heating elements (ref. 3). This ease of instrumentation made it possible to obtain more measurements in regions of steep temperature gradients and thus to determine better the wall temperature profile.

At present, the main disadvantage in using a tungsten honeycomb heater, rather than a parallel flat-plate or a mesh-type heater, is the high initial cost. However, as the tungsten fabrication technology advances, the tungsten honeycomb heaters will probably become more economical. When it is used with nonoxidizing gases, a honeycomb heating element has many advantages over both the parallel flat-plate and mesh-type heaters. Some of these advantages are listed as follows:

(1) A strong structure for a given surface- to-volume ratio.
No spacers are required as supports; thus, less pressure drop occurs for a given mass velocity and $L/D_e$.

(2) Continuous flow passages along the length of the test section, which prevents cross flow between passages.
No outside insulating housing is needed to surround the test section; consequently, a higher outlet gas temperature can be obtained for a given maximum surface temperature.

(3) Relative thermal expansion between insulating housing and heater element is not a concern.
No insulating housing is required.

# REFERENCES

1. Slaby, Jack G.; Maag, William L.; and Siegel, Byron L.: Laminar and Turbulent Hydrogen Heat Transfer and Friction Coefficients Over Parallel Plates at 5000° R. NASA TN D-2435, 1964.

2. Slaby, Jack G.; Siegel, Byron L.; Mattson, William F.; and Maag, William L.: A 4500° R (2500° K) Flowing-Gas Facility. NASA TM X-1506, 1968.

3. Siegel, Byron L.: Design and Operation of a High-Temperature Tungsten-Mesh Gas Heater. NASA TM X-1466, 1967.

4. Weast, Robert C., ed.: Handbook of Chemistry and Physics. 37th ed., Chemical Rubber Publ. Co., 1955, p. 2360.

5. Keenan, Joseph H.; Kaye, Joseph: Gas Tables - Thermodynamic Properties of Air, Productions of Combustion and Component Gases and Compressible Flow Functions. John Wiley & Sons, Inc., 1948.

6. Svehla, Roger A.: Estimated Viscosities and Thermal Conductivities of Gases at High Temperatures. NASA TR R-132, 1962.

7. Grier, Norman T.: Calculation of Transport Properties and Heat-Transfer Parameters of Dissociating Hydrogen. NASA TN D-1406, 1962.

8. Humble, Leroy V.; Lowdermilk, Warren H.; and Desmon, Leland G.: Measurements of Average Heat-Transfer and Friction Coefficients for Subsonic Flow of Air in Smooth Tubes at High Surface and Fluid Temperatures. NACA Rep. 1020, 1951.

9. Taylor, Maynard F.: Correlation of Local Heat Transfer Coefficients for Single Phase Turbulent Flow of Hydrogen in Tubes with Temperature Ratios to 23. NASA TN D-4332, 1968.

10. Deissler, Robert G.; and Taylor, Maynard F.: Analysis of Turbulent Flow and Heat Transfer in Noncircular Passages. NASA TR R-31, 1959.

11. Reshotko, Meyer: Flow and Wall-Temperature Sensitivity in Parallel Passages for Large Inlet to Exit Density Ratios in Subsonic Flow. NASA TN D-4649, 1968.

*"The aeronautical and space activities of the United States shall be conducted so as to contribute . . . to the expansion of human knowledge of phenomena in the atmosphere and space. The Administration shall provide for the widest practicable and appropriate dissemination of information concerning its activities and the results thereof."*

— NATIONAL AERONAUTICS AND SPACE ACT OF 1958

# NASA SCIENTIFIC AND TECHNICAL PUBLICATIONS

TECHNICAL REPORTS: Scientific and technical information considered important, complete, and a lasting contribution to existing knowledge.

TECHNICAL NOTES: Information less broad in scope but nevertheless of importance as a contribution to existing knowledge.

TECHNICAL MEMORANDUMS: Information receiving limited distribution because of preliminary data, security classification, or other reasons.

CONTRACTOR REPORTS: Scientific and technical information generated under a NASA contract or grant and considered an important contribution to existing knowledge.

TECHNICAL TRANSLATIONS: Information published in a foreign language considered to merit NASA distribution in English.

SPECIAL PUBLICATIONS: Information derived from or of value to NASA activities. Publications include conference proceedings, monographs, data compilations, handbooks, sourcebooks, and special bibliographies.

TECHNOLOGY UTILIZATION PUBLICATIONS: Information on technology used by NASA that may be of particular interest in commercial and other non-aerospace applications. Publications include Tech Briefs, Technology Utilization Reports and Notes, and Technology Surveys.

*Details on the availability of these publications may be obtained from:*

## SCIENTIFIC AND TECHNICAL INFORMATION DIVISION

# NATIONAL AERONAUTICS AND SPACE ADMINISTRATION
### Washington, D.C. 20546